

Synthesis, structural study and electrochemical properties of copper(II) complexes derived from benzene- and *p*-toluenesulphonylhydrazones

L. LARABI^a, Y. HAREK^{a*}, A. REGUIG^a and M. M. MOSTAFA^b

^aChemistry Department, Faculty of Science, Tlemcen University, Tlemcen, Algeria and ^bChemistry Department, Faculty of Science, Mansoura University, Mansoura, Egypt

(Received 12 February, revised 9 September 2002)

Abstract: The synthesis and characterization of benzene- and *p*-toluenesulphonylhydrazones derived from salicylaldehyde and 2-hydroxy-1-naphthaldehyde and their Cu(II) complexes are reported. The compounds were characterized on the basis of elemental analyses, electronic and IR spectra, magnetic moments, and conductance measurements. The electrochemical behavior of the Cu(II) complexes was investigated in DMSO by cyclic voltammetry (CV), rotating disc electrode (RDE) and coulometry. The oxidative polymerization of the copper complexes on a glassy carbon electrode was carried out in DMSO.

Keywords: sulphonylhydrazone-Cu(II) complex, cyclic voltammetry.

INTRODUCTION

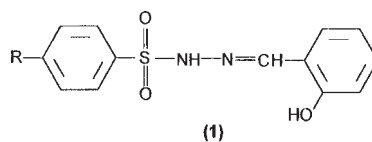
The use of benzene- and *p*-toluenesulphonylhydrazines and their hydrazones derivatives as ligands for transition metal ions has received considerable attention because of their photochromic effect.^{1–5} Due to their biological significance as models of redox enzymes, the coordination chemistry of high oxidation state transition-metal complexes is an area of great importance. Investigations to assess the possible use of metal chelates in the stabilization of unusual high oxidation states has been described in the literature.^{6–9}

In a continuation of our earlier studies,^{10,11} we report herein the synthesis, electrochemical properties, and electrooxidative polymerization of copper(II) complexes with salicylaldehyde benzenesulphonylhydrazone (SBSH), 2-hydroxy-1-naphthaldehyde benzenesulphonylhydrazone (NBSH), salicylaldehyde *p*-toluenesulphonylhydrazone (STSH), and 2-hydroxy-1-naphthaldehyde *p*-toluenesulphonylhydrazone (NSTH) (Scheme 1). The capacity of these chelating ligands to stabilize copper(III) complexes was also explored.

EXPERIMENTAL

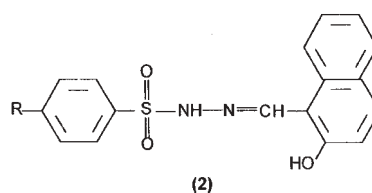
All the chemicals used for the preparation of the ligands were BDH quality. Magnetic susceptibilities were determined using a Johnson Matthey balance at room temperature (25 °C) with Hg[Co(SCN)₄] as the standard. C,

* Author for correspondence (e-mail: y_harek@mail.univ-tlemce.dz)



SBSH (H₂L₁): R = H

STSH (H₂L₃): R = CH₃



NBSH (H₂L₂): R = H

NTSH (H₂L₄): R = CH₃

Scheme 1.

H, and N contents were determined at the Micro-analytical unit, Cairo University, Egypt. IR spectra were recorded in KBr and/or Nujol mull on a Perkin Elmer PE 983 spectrometer and the electronic spectra were recorded in Nujol and in DMF on a Perkin-Elmer model 550-S spectrometer. The conductivity measurements were carried out in DMF (*ca.* 10⁻³ M) using a Tacussel conductivity bridge model 75. The electrochemical experiments were performed using a Trace-lab50 from Radiometer which includes a polarographic analyzer (Pol 150), a polarographic stand (MDE 150), and trace Master 5 software. Cyclic voltammetry was performed using a conventional three-electrode system. The working electrode was a pre-polished glassy carbon (GC.) disc of 3 mm diameter (Radiometer). Potentials are expressed *versus* the Ag/AgCl (KCl, 3M) electrode separated from the test solution by a salt bridge containing the solvent / supporting electrolyte. The auxiliary electrode was a platinum wire. The RDE study was performed using Radiometer model BM-EDI101 rotating disc electrode. The rotating speed ω was regulated by an Asservitex Model CTV101 from Radiometer.

The following solutions were studied: 0.5, 1.0, 1.5, 2.0, 3.0 and 4.0 mM of complexes in DMSO and 0.1 M N(Et)₄ClO₄ as supporting electrolyte. The RDE voltammograms were recorded in each solution, using a scan rate of 10 mV/s and rotating speeds ω of 25, 50, 75, 100, 150, 200, 300 and 400 rpm. In the CV measurements, scan rates ν of 0.010, 0.025, 0.050, 0.100, 0.200, 0.400, 0.500, 1.000 and 2.000 V/s were employed. All experiments were carried out at 25 °C \pm 0.1 using a Julabo thermostat. In the coulometric experiments, the auxiliary electrode was separated from the solution by a glass frit disk and the working electrode was controlled by a Radiometer PGP201 potentiostat.

Synthesis of ligands

Benzene- and *p*-toluenesulphonylhydrazine (BSH, TSH) were prepared as reported earlier.^{12,13} The ligands SBSH, NBSH, STSH, and NTSH were isolated by refluxing equimolar amounts of BSH, TSH with salicylaldehyde and/or 2-hydroxy-1-naphthaldehyde in absolute ethanol for two hours and in the presence of two drops of glacial acetic acid. The products were crystallized from ethanol (80 %). The purity of the ligands was checked by elemental analyses and TLC.

Synthesis of the complexes

The metal complexes were prepared by a general method. A hot absolute EtOH solution of Cu(II) acetate (1 mmol) was added to a hot solution of the corresponding ligand (2 mmol) in EtOH under continuous stirring. The precipitated complex was filtered off hot, washed several times with absolute EtOH and dried in a desiccator over silica gel.

[Cu₂(HL₁)₂(OAc)₂]. M.p: 250 °C, IR $\nu(\text{cm}^{-1})$ 1600 (C=N), 1440 (OAc), 495 (SO₂), 3160 (NH). Anal. Calcd. for C₃₀H₂₈N₄O₁₀S₂Cu₂: C, 45.3; H, 3.5; N, 7.0; Cu, 15.9%. Found: C, 46.1; H, 3.1; N, 8.0; Cu, 15.4%.

[Cu(HL₂)₂]. M.p: 228 °C, IR $\nu(\text{cm}^{-1})$ 1600 (C=N), 550 (SO₂), 3180 (NH). Anal. Calcd. for C₃₄H₂₆N₄O₆S₂Cu: C, 57.2; H, 3.7; N, 7.7; Cu, 8.9%. Found: C, 56.3; H, 3.6; N, 7.7; Cu, 9.3%.

[Cu(HL₃)₂]. M.p: 225 °C, IR $\nu(\text{cm}^{-1})$ 1600 (C=N), 500 (SO₂), 3200 (NH). Anal. Calcd. for C₂₈H₂₆N₄O₆S₂Cu: C, 52.4; H, 4.1; N, 8.7; Cu, 9.9%. Found: C, 52.3; H, 3.8; N, 8.8; Cu, 10.5%.

[Cu(HL₄)₂]. M.p: 229 °C, IR $\nu(\text{cm}^{-1})$ 1600 (C=N), 495 (SO₂), 3200 (NH). Anal. Calcd. for C₃₆H₃₀N₄O₆S₂Cu: C, 58.0; H, 4.1; N, 7.5; Cu, 8.6%. Found: C, 58.0; H, 3.7; N, 7.5; Cu, 9.3%.

RESULTS AND DISCUSSION

Electronic spectra nad magnetic studies

The electronic spectra of H₂L₁ and H₂L₃ in acetone show four bands. H₂L₁ exhibits bands at 438, 370, 330, and 304 nm while H₂L₃ shows bands at 430, 412, 380, and 340 nm. These bands can be assigned to $n \rightarrow \pi^*$ (SO₂), $n \rightarrow \pi^*$ (C=N), $\pi \rightarrow \pi^*$ (SO₂), and $\pi \rightarrow \pi^*$ (C=N), respectively.¹⁴ On the other hand, the electronic spectra of H₂L₂ and H₂L₄ in acetone exhibit five bands. H₂L₂ shows bands at 450, 418, 376, 360, and 330 nm while H₂L₄ exhibits bands at 450, 438, 380, 360, and 328 nm. These bands may be assigned to $n \rightarrow \pi^*$ (SO₂), $n \rightarrow \pi^*$ (C=N), $\pi \rightarrow \pi^*$ (SO₂), $\pi \rightarrow \pi^*$ (C=N), and $\pi \rightarrow \pi^*$ (naphthyl), respectively.¹⁴ The electronic spectra of [Cu₂(HL₁)₂(OAc)₂] show two bands at 770 and 550 nm which may be assigned to ${}^2B_{1g} \rightarrow {}^2E_{1g}$ and ${}^2B_{1g} \rightarrow {}^2A_{1g}$, which is consistent with a square planar structure.¹⁵ The magnetic moment for this complex (0.89 B.M.) is much lower than the normal value, may be due to a strong Cu–Cu interaction,¹⁶ indicating the dimeric nature of this complex. [Cu(HL₂)₂] is characterized by four bands at 790, 640, 510, and 474 nm. The last band is attributed to charge transfer. This suggests a deformed tetrahedral structure around the Cu(II) ion.^{17,18} The magnetic moment of [Cu(HL₂)₂] is 1.73 B.M. This result proves the absence of a Cu–Cu interaction, indicating the monomeric nature of this complex. The electronic spectrum of [Cu(HL₃)₂] exhibits an intense band at *ca.* 690 nm with a shoulder at 650 nm. This observation together with the magnetic moment (1.95 B.M.) support the presence of a square-planar environment around the Cu(II) ion.¹⁵ The electronic spectrum of [Cu(HL₄)₂] is similar to that of [Cu(HL₂)₂].

IR spectra and conductivity studies

In the IR spectra of the complexes, the stretching vibration of the free ligands ($\nu(\text{OH})$, 3020–3460 cm^{-1}) is not observed, suggesting deprotonation of the hydroxy group and formation of M–O bonds.^{19,20} Bands near 1620 cm^{-1} in the free ligands are assigned to $\nu(\text{C=N})$. These bands are shifted to lower wave numbers in the complexes due to the coordination of the nitrogen atom of the azomethine group to the metal ion. The bands assignable to $\nu(\text{SO}_2)$ are not shifted in the complexes. The bands observed for the complexes between 560–520 and 430–410 cm^{-1} were metal sensitive and are assigned to $\nu(\text{M-O})$ and $\nu(\text{M-N})$,²¹ respectively. Moreover, the test for OH groups (spot test technique²²) was negative.

The molar conductivities of the complexes in DMF (25 °C) are in the 3.0 to 7.0 $\Omega^{-1} \text{cm}^2 \text{mol}^{-1}$ range, indicating their non-electrolytic nature.²³

Electrochemical study

CV and RDE studies. The electrochemical properties of complexes at different concentrations were studied in DMSO containing 0.1 M $\text{N}(\text{Et})_4\text{ClO}_4$ as supporting electrolyte. The electrochemical behavior of $[\text{Cu}_2(\text{HL}_1)_2(\text{OAc})_2]$ is shown in Fig. 1a and is similar to that of $[\text{Cu}_2(\text{HL}_3)_2]$, Fig. 1b. In the first anodic scan (Fig. 1a), the CV displays two waves at E_{pa} values 0.91 V (peak 1) and 1.44 V (peak 2), respectively. Peak 1 is assigned to the oxidation of the central metal of $[\text{Cu}_2(\text{HL}_1)_2(\text{OAc})_2]$. The observed CV implies that both Cu(II) centers of $[\text{Cu}_2(\text{HL}_1)_2(\text{OAc})_2]$ simultaneously ex-

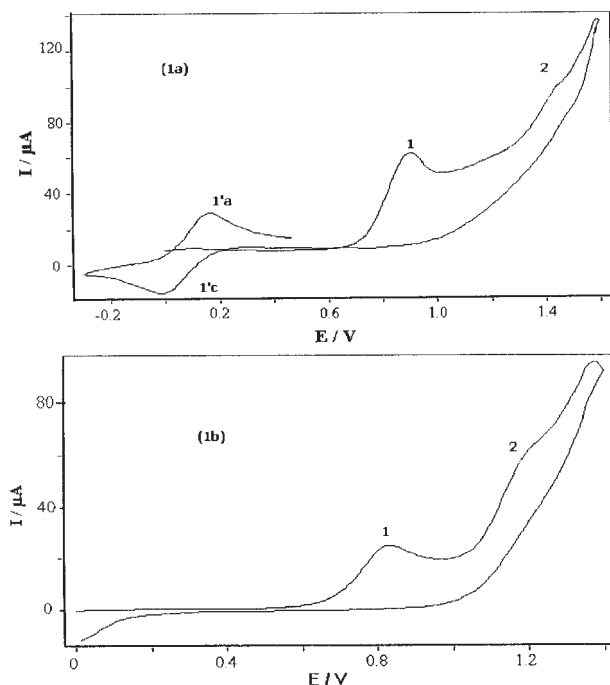


Fig. 1. Cyclic voltammogram of 2 mM $[\text{Cu}_2(\text{HL}_1)_2(\text{OAc})_2]$ (a) and 2 mM $[\text{Cu}(\text{HL}_3)_2]$ (b) in DMSO- $\text{N}(\text{Et})_4\text{ClO}_4$ (0.1 M) at GCE; scan rate 0.1 V/s.

change electrons with the electrode. On the other hand, peak 2 is observed at nearly the same potential value as the corresponding ligand (H_2L_1) and may be assigned to the irreversible oxidation of the NH - group. When the potential scan in the positive direction is reversed at 1.6 V or 1.4 V (Fig. 1a and 1b), a new reduction peak appears in the second scan at a peak potential -0.02 V (peak 1'c). Reversal of the scan at 0.9 V again gives rise to the appearance of peak 1'c, suggesting the association of peaks 1 and 1'c. On the other hand, peak 1'c is associated with an oxidative peak 1'a, which appears when the potential scan in the negative direction is reversed at -0.3 V. Therefore, peak 1'c can be attributed to the reduction of a product formed during the chemical reaction coupled to the electrochemical process: $\text{Cu}(\text{II}) \rightarrow \text{Cu}(\text{III})$. Since the principal goal of

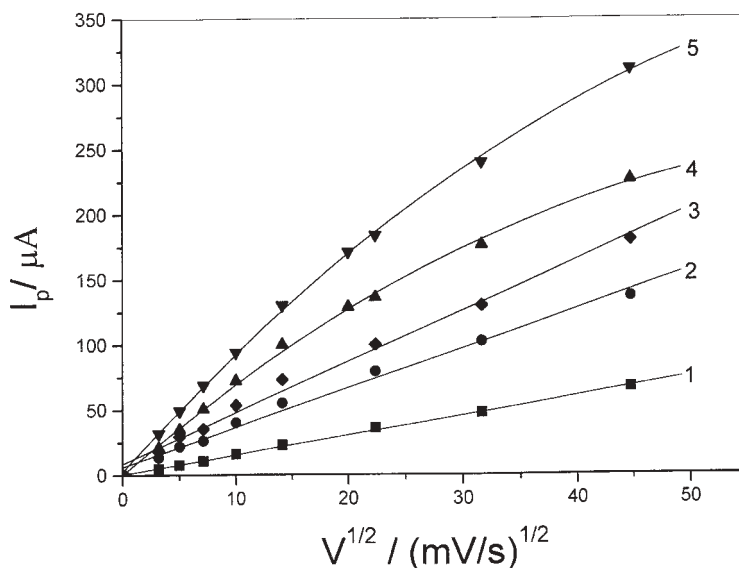


Fig. 2. Variation of the anodic peak currents, I_{pa1} , versus $v^{1/2}$ for various $[\text{Cu}_2(\text{HL}_1)_2(\text{OAc})_2]$ concentrations: (1) 0.5 mM; (2) 1.5 mM; (3) 2.0 mM; (4) 3.0 mM; (5) 4.0 mM.

this study was to investigate the peak 1 process, which is the only peak arising directly from the oxidation of Cu(II), further details concerning the other peaks will not be presented here. The electrochemical irreversibility of this process was confirmed by the fact that, in the range of sweep rates from 10 to 2000 mV/s, the slope $\Delta E/\Delta \log v$ (for $[\text{Cu}_2(\text{HL}_1)_2(\text{OAc})_2]$) has a value of 0.052 V, which is larger than those expected for reversible processes. Furthermore, the oxidation peak currents (i_{pa1}) of $[\text{Cu}_2(\text{HL}_1)_2(\text{OAc})_2]$ were linear with $v^{1/2}$ over the entire range of studied sweep rates at a complex concentration ≤ 2 mM. At higher complex concentration and for $v > 400$ mV/s, this increase was less than linear (Fig. 2). These results indicate that the oxidation of the complex occurs *via* an irreversible electron transfer followed by a chemical reaction. In the case that the oxidation of $[\text{Cu}_2(\text{HL}_1)_2(\text{OAc})_2]$ at the surface electrode is controlled solely by a mass-transfer process in the solution, the relation between the limiting current and the rotation speed should obey the Levich equation:

$$I_1 = 0.620 n F A D^{2/3} v^{-1/6} \omega^{1/2} c_0, \quad (1)$$

where D , v , ω and c_0 are the diffusion coefficient, the kinematic viscosity, the rotation speed and the bulk concentration of the reactant in the solution, respectively, and all other parameters have their conventional meanings. On the basis of Eq. (1), a plot of the limiting current, I_1 as a function of $\omega^{1/2}$ should be a straight line. This was the case when the complex concentration was lower than 2 mM (Fig. 3). For complex concentrations higher than 2 mM, as can be seen from the Levich plot shown in Fig. 3, the current increases with increasing rotation speed of the electrode, but was found to be of curved shape, indicating kinetic limitation. The behavior of the oxidation peak currents (I_{pa1}) of $[\text{Cu}(\text{HL}_3)_2]$ and the I_1

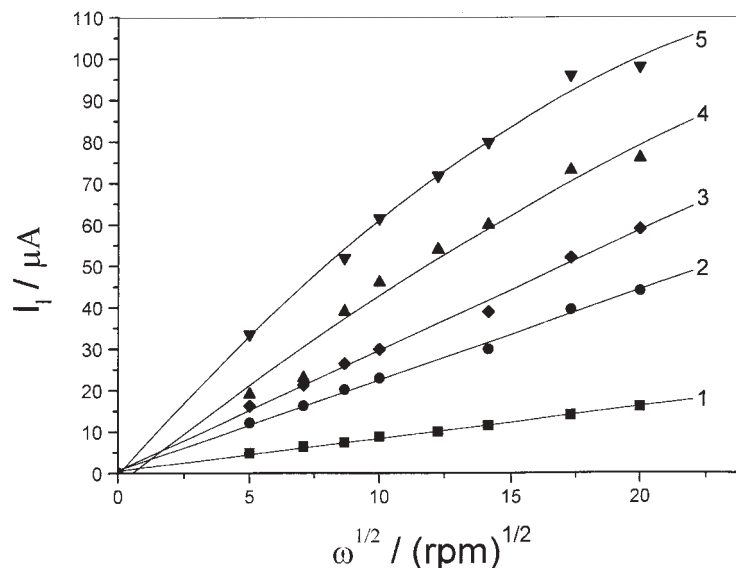


Fig. 3. Levich plots of the first anodic limiting current of $[\text{Cu}_2(\text{HL}_1)_2(\text{OAc})_2]$ at different concentrations: (1) 0.5 mM; (2) 1.5 mM; (3) 2 mM; (4) 3 mM; (5) 4 mM at a GCE; $v = 10$ mV/s.

v vs $\omega^{1/2}$ equations are identical to the behavior reported for CV and RDE studies of $[\text{Cu}_2(\text{HL}_1)_2(\text{OAc})_2]$. A typical cyclic voltammetric response of $[\text{Cu}(\text{HL}_2)_2]$ is shown in Fig. 4. The cyclic voltammogram of $[\text{Cu}(\text{HL}_2)_2]$ is similar to that of $[\text{Cu}(\text{HL}_4)_2]$. In the anodic direction, the cyclic voltammograms of $[\text{Cu}(\text{HL}_2)_2]$ and $[\text{Cu}(\text{HL}_4)_2]$ exhibit three oxidation peaks (1, 3, and 2) at 25 °C at a sweep rate of 0.1 V/s. The anodic peak 1 is coupled with the cathodic peak 1'c. Reversal of the scan at 1.1 V gives rise to the appearance of peaks 3'c and 3''c, indicating the association of these peaks and peak 3. Moreover, the peak 3 is observed at the same potential value as the corresponding ligands H_2L_2 and H_2L_4 and is tentatively attributed to the irreversible oxidation of the naphthyl group. The peak current I_p , for the oxidation peak 1 increased linearly with bulk solution concentration of $[\text{Cu}(\text{HL}_2)_2]$ over the concentration range 0.5 to 2 mM. At concentrations higher than 2 mM, this increase was less than linear. Furthermore, it was shown that I_p increases linearly as a function of the square root of the voltage sweep rate over the sweep rate range 0.01 to 2 V/s at complex concentrations ≤ 2 mM. At higher concentrations, the current increases with increasing voltage sweep rate, but was found to be nonlinear.

Moreover, the RDE study showed that for complex concentrations ≤ 2 mM, the limiting current increases linearly with increasing rotation speed of the electrode. At higher complex concentrations, this increase was found to be curved shape. This behavior indicates that the peak 1 oxidation of $[\text{Cu}(\text{HL}_2)_2]$ is a diffusion controlled reaction over the entire range of studied voltage sweep rates at complex concentrations ≤ 2 mM. At higher complex concentration (> 2 mM), the current is controlled by the rate of charge transfer or of a chemical reaction.

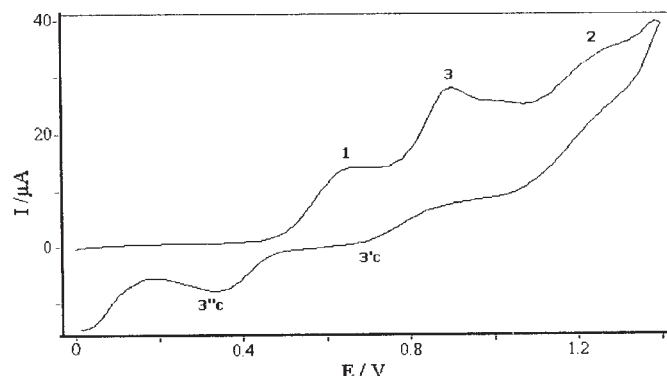


Fig. 4. Cyclic voltammogram of 2 mM $[\text{Cu}_2(\text{HL}_2)_2]$ in DMSO- $\text{N}(\text{Et})_4\text{ClO}_4$ (0.1 M) at a GCE; scan rate 0.1 V/s, scan from 0 to +1.4 V.

The electrochemical data of the 2 mM solutions of the studied copper complexes are summarized in Table I. A shift in the formal potentials of the copper(III) / copper(II) couples to more negative values, *i.e.*, the stabilization of the higher oxidation state, which occurs upon ligand substitution along this series can also be registered. A comparison of the redox potentials of the $[\text{Cu}(\text{HL}_3)_2]$ and $[\text{Cu}(\text{HL}_4)_2]$ complexes where both ligands H_2L_3 and H_2L_4 have the same set of donor atoms but differ in the size of central chelating agents shows that the copper(III) complex $[\text{Cu}(\text{HL}_4)_2]$ is thermodynamically more stable, *i.e.*, the Cu(III) – Cu(II) potential is lowered by 180 mV. Substitution of the phenyl by naphthyl fragment causes a large enough increase in aromatic character to produce the observed negative shift in the formal potential. Hence, the electron density at the metal center is enhanced as the aromatic character is increased, thus facilitating its oxidation. Generally, an increase in the overall stability of the copper(III) complex is to be expected, which would result in a decrease in the Cu(III) – Cu(II) potential, as was experimentally confirmed. Otherwise, a comparison of the redox potentials of the $[\text{Cu}(\text{HL}_2)_2]$ and $[\text{Cu}(\text{HL}_4)_2]$ shows a small negative shift of the Cu(III) – Cu(II) potential, indicating a weak effect of the CH_3 group.

TABLE I. Cyclic voltammetric data of the studied complexes*

| Complex | E_p/V | | | | | | |
|--|--------------------|--------------------|--------------------|-----------------------------|-----------------------------|-----------------------------|------------------------------|
| | $E_{\text{pa}}(1)$ | $E_{\text{pa}}(2)$ | $E_{\text{pa}}(3)$ | $E_{\text{pa}}(1'\text{a})$ | $E_{\text{pc}}(1'\text{c})$ | $E_{\text{pc}}(3'\text{c})$ | $E_{\text{pc}}(3''\text{c})$ |
| $[\text{Cu}_2(\text{HL}_1)_2(\text{OAc})_2]$ | 0.91 | 1.44 | – | 0.16 | –0.02 | – | – |
| $[\text{Cu}(\text{HL}_2)_2]$ | 0.68 | 1.28 | 0.98 | 0.13 | 0.02 | 0.76 | 0.24 |
| $[\text{Cu}(\text{HL}_3)_2]$ | 0.83 | 1.21 | – | 0.17 | 0.03 | – | – |
| $[\text{Cu}(\text{HL}_4)_2]$ | 0.65 | 1.27 | 0.91 | 0.13 | 0.03 | 0.71 | 0.19 |

* $c = 2 \times 10^{-3} \text{ mol/dm}^3$ in DMSO solution (0.1 M $\text{N}(\text{Et})_4\text{ClO}_4$), E values (V versus $\text{Ag}/\text{AgCl}/3\text{M KCl}$). Scan rate 100 mV/s; E_{pa} and E_{pc} are the anodic and cathodic peak potentials, respectively.

Coulometric oxidation and characterization of the generated species. Exhaustive oxidation of $[\text{Cu}_2(\text{HL}_1)_2(\text{OAc})_2]$ and $[\text{Cu}(\text{HL}_2)_2]$ carried out at a constant potential (1000 mV

for the former and 750 mV for the latter) indicate that 1.7 electrons and 0.9 electron were transferred per molecule, respectively. The logarithmic analysis ($\log I - \log t$) of the coulometric curves was not linear. This is consistent with the presence of a chemical step after the electron transfer. After exhaustive oxidation of a complex, the resulting solution was scanned from 0 to 1200 mV. None of the oxidized complexes exhibited an oxidation signal $\text{Cu(II)} \rightarrow \text{Cu(III)}$, whereas the cathodic peak 1'c appeared again.

The UV-visible electronic absorption spectrum of the copper(III) complex obtained electrochemically (by exhaustive oxidation of $[\text{Cu}(\text{HL}_2)_2]$) consists of an intense band in the UV region centered at 347 nm, with three distinct shoulders located at 360, 410, and 520 nm. The high-energy peak, which also appears in the spectrum of the copper(II) complex as a single band with small shift and almost the same intensity, is commonly assigned to a $\pi-\pi^*$ transition within the aromatic ring of the ligand, while the weak shoulders on the low-energy tail of this intra-ligand absorption band may then originate from d-d transitions. It is known that three transitions are expected for a diamagnetic copper(III) ion with a d^8 electronic configuration in a square-planar environment.⁸ Note that with respect to the original Cu(II) complex, the bands at 398 and 417 nm, which may be attributed to ligand to metal charge transfer absorption bands, and the broad bands at 485 and 700 nm, which may originate from d-d transitions, disappeared.

The electronic spectrum of the electrochemically generated copper(III)- H_2L_1 complex in DMSO exhibits the above mentioned intra-ligand band at 317 nm and two very broad bands at 380 and 760 nm. The electronic spectrum of $[\text{Cu}_2(\text{HL}_1)_2(\text{OAc})_2]$ complex in DMSO shows four bands at 320, 367, 398, and 420 nm, assignable to the $\pi-\pi^*$ transition within the naphthyl ring, to acetate-to-copper(II) charge transfer and to ligand H_2L_1 -to-Cu(II) LMCT transitions, respectively. It also exhibits two broad d-d transitions at 487 and 710 nm.¹⁵

Comparison of the electronic spectrum of the electrochemically generated copper(III) - H_2L_1 and that of $[\text{Cu}_2(\text{HL}_1)_2(\text{OAc})_2]$ shows the absence of LMCT transitions in the former. This result indicates that the energy of the transitions increases with increasing oxidation state of the central metal, as is mentioned in the literature.¹⁵ It

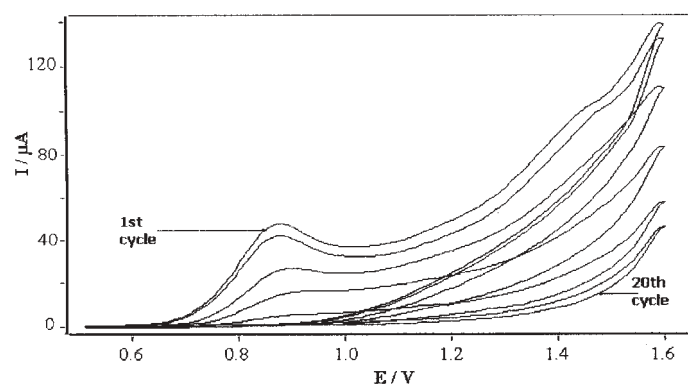


Fig. 5. Consecutive cyclic voltammograms of 2 mM $[\text{Cu}_2(\text{HL}_1)_2(\text{OAc})_2]$ in DMSO - $\text{N}(\text{Et})_4\text{ClO}_4$ (0.1 M) at a GCE; scan rate 0.1 V/s, scan from 0 to +1.6 V.

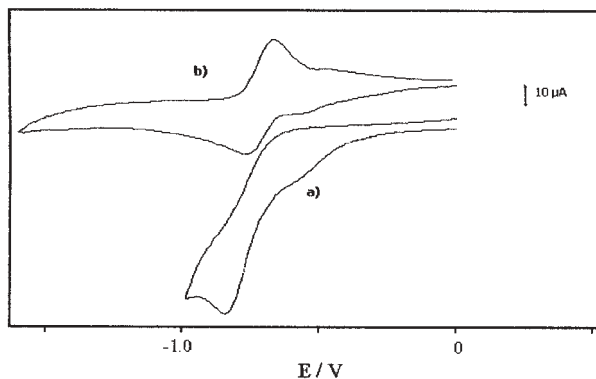


Fig. 6. Cyclic voltammograms (0.1 V/s) of 2 mM solution of $[\text{Cu}_2(\text{HL}_1)_2(\text{OAc})]$ in $\text{DMSO}-\text{N}(\text{Et})_4\text{ClO}_4$ (0.1 M): a) at bare GCE and b) at GCE modified with the electropolymerized film of $[\text{Cu}_2(\text{HL}_1)_2(\text{OAc})]$.

may also indicate the partial dissociation of the complex obtained by exhaustive coulometry. Note that the higher aromaticity of the naphthyl ring of H_2L_2 relative to the phenyl ring of H_2L_1 is presumably responsible for the bathochromic shift of the high energy band of $[\text{Cu}(\text{HL}_2)_2]$ compared to that of $[\text{Cu}_2(\text{HL}_1)_2(\text{OAc})_2]$.

Therefore, it is possible to suggest that the generated Cu(III) complexes undergo fast chemical reaction subsequent to electron transfer which probably results in the partial dissociation of the complexes.

Electro-oxidative polymerization. The cyclic voltammograms of the $[\text{Cu}_2(\text{HL}_1)_2(\text{OAc})_2]$ complex, in DMSO, during repeated potential scans in the 0.0 V to 1.6 V range are shown in Fig. 5. These CVs are similar to those of the $[\text{Cu}(\text{HL}_3)_2]$ complex. Oxidation of the former complex is observed during the first positive scan at 0.91 V and 1.44 V. Consecutive recordings show a decrease in the peak current. This indicates that a polymeric film is formed on the electrode as a result of oxidation and that the film is a poor conductor in this potential range.²⁴ After deposition and careful rinsing, the electrode was transferred to a fresh aerated monomer-free electrolyte solution. The cyclic voltammogram of this modified electrode displayed an irrevers-

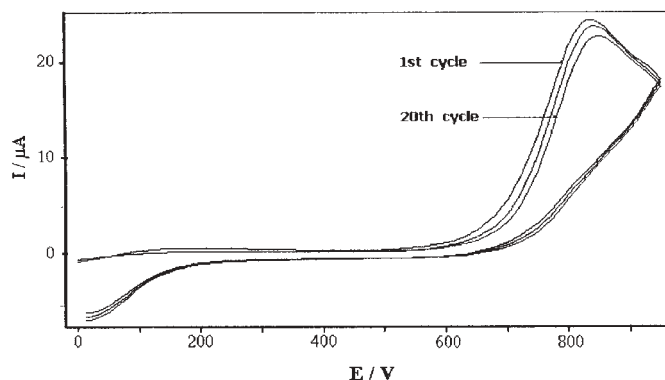


Fig. 7. Consecutive cyclic voltammogram of 2 mM $[\text{Cu}_2(\text{HL}_1)_2(\text{OAc})_2]$ in $\text{DMSO}-\text{N}(\text{Et})_4\text{ClO}_4$ (0.1 M) at a GCE; scan rate 0.1 V/s, scan from 0 to +0.9 V.

ible cathodic wave at -560 mV, which can be ascribed to the Cu(II) / Cu(I) process and a well-defined pair of peaks at $E^0 = (E_{pc} + E_{pa}) / 2 = -0.72$ V, which can be attributed to the reduction of oxygen, Fig. 6b. Comparison of Fig. 6a and Fig. 6b shows that the electrode modified with a film of electropolymerized $[Cu_2(HL_1)_2(OAc)_2]$ facilitates the reduction of oxygen. A decrease of *ca.* 80 mV can be observed in the overpotential of oxygen reduction for the modified electrode relative to the bare electrode. Fig. 6 also shows that the reversibility of oxygen reduction increases significantly for the modified electrode relative to the bare electrode.

Figure 7 shows that when the potential cycling was confined between the potential limits of 0.0 V and 0.9 V no polymer was formed. This result indicates that the oxidation of NH-groups at 1.2 V is responsible for the electropolymerization of the monomer complex. However, no polymer was formed on the electrode during repetitive potential scans of the ligand H_2L_1 in the 0 to 1.4 V range, suggesting that electropolymerization is due to the oxidation of the ligand complexed with copper ion. The polymer formed adheres to the glassy carbon electrode and is a poor conductor in the above potential range. However, when the potential is scanned in the cathodic direction (< -1 V), a reductive degradation of the polymer layers occurs. This is obvious from the increase of the height of the irreversible redox peaks (1 and 3) after the negative scan to potentials less negative than -1 V.

Furthermore, consecutive potential scans of $[Cu(HL_1)_2]$ and $[Cu(HL_4)_2]$ in the 0 to 1.4 V range do not lead to the electropolymerization of these complexes.

Acknowledgements: The authors are indebted to the A. N. D. R. U. and the Ministère de l'Enseignement Supérieur et de la Recherche Scientifique (ALGERIE) for financial support.

ИЗВОД

СИНТЕЗЕ, СТРУКТУРЕ И ЕЛЕКТРОХЕМИЈСКЕ ОСОБИНЕ БАКАР(II) КОМПЛЕКСА СА БЕНЗЕН- И *p*-ТОЛУЕНСУЛФОНИЛХИДРАЗОНИМА

L. LARABI^a, Y. HAREK^a, A. REGUIG^a and M. M. MOSTAFA^b

^aChemistry Department, Faculty of Science, Tlemcen University, Tlemcen, Algeria and ^bChemistry Department, Faculty of Science, Mansoura University, Mansoura, Egypt

Приказане су синтезе и карактеризације бензен- и *p*-толуенсулфонилхидразона добијених од салицилалдехида и 2-хидрокси-1-нафталдехида као и њихови Cu(II) комплекси. Карактерисање једињења изведено је на основу елементарне анализе, електронских и IR спектара, магнетних момената и проводљивости. Електрохемијско понашање Cu(II) комплекса проучавано је цикличном волтаметријом у DMSO ротирајућом диск електродом, као и кулометријски. Оксидативна полимеризација комплекса бакра на електроди од стакластог карбона вршена је у DMSO.

(Примљено 12. фебруара, ревидирано 9. септембра 2002)

REFERENCES

1. L. Friedman, R. L. Litle, W. R. Rechile, *Org. Synth. Collect.* **5** (1973) 1055
2. M. T. Bogert, A. Stull, *Org. Synth. Collect.* **1** (1941) 220
3. E. Wertheim, *Org. Synth. Collect.* **2** (1961) 471
4. J. L. Wang, F. N. Bruscatto, *Tetrahedron Lett.* (1968) 4593

5. E. Hadjoudis, D. G. Hadjoudis, *Chim. Chronica. New Series* **4** (1975) 51
6. D. W. Wargerum, K. L. Chellapa, G. L. Burce, *J. Am. Chem. Soc.* **97** (1975) 6894
7. J. J. Bour, P. J. M. W. L. Birker, J. J. Steggerda, *Inorg. Chem.* **10** (1971) 1202
8. R. Ruiz, C. Surville - Barland, A. Aukauloo, E. Anxolabehere - Mallart, Y. Journaux, J. Cano, M. C. Munoz, *J. Chem. Soc., Dalton Trans.* (1997) 745
9. B. Cervera, J. L. Sanz, M. J. Ilbanes, G. Vila, F. L. Loret, M. Julve, R. Ruiz, X. Ottenwaelder, S. Poussereau, Y. Journaux, M. C. Munoz, *J. Chem. Soc., Dalton Trans.* (1998) 781
10. T. H. Rakha, A. A. El Asmy, M. M. Mostafa, A. G. Kourshy, *Trans. Met. Chem.* **12** (1987) 125
11. A. Reguig, A. K. T. Maki, M. M. Mostafa, *Proc. First Intern. Sci. Conference (Science and Development)* Cairo, 20–23 March, (1995) 135–140
12. A. I. Vogel, *Text Book of Practical Organic Chemistry*, 4th Ed. Longman, New York, 1978
13. A. Albert, R. Roger, *J. Chem. Soc.* (1949) 1148
14. C. N. R. Rao, *Ultraviolet and Visible Spectroscopy*, Plenum press, New York, 1975
15. A. B. P. Lever, *Inorganic Electronic Spectroscopy*, Elsevier, Amsterdam, 1968
16. M. Kato, K. B. Jonassen, J. C. Fanning, *Chem. Rev.* **64** (1964) 99
17. E. Pappalardo, *J. Mol. Spectroscopy* **6** (1961) 554
18. O. G. Holmes, D. S. Mc Clure, *J. Chem. Phys.* **26** (1957) 2552
19. S. K. Bansal, S. Tikku, R. S. Sindhu, *J. Ind. Chem. Soc.* **68** (1991) 566
20. W. P. Griffith, S. I. Mostafa, *Polyhedron* **11** (1992) 2997
21. J. R. Ferraro, *Low Frequency Vibrations of Inorganic and Coordination Compounds*, Plenum Press, New York, 1971
22. R. Feigl, *Spot Tests in Organic Analysis*, Elsevier, Amsterdam, 1966
23. W. J. Geary, *Coord. Chem. Revs.* **7** (1971) 81
24. J. Losada, I. Del Peso, *Trans. Met. Chem.* **25** (2000) 112.